

FTUV/98-79
IFIC/98-80

NLO CALCULATIONS OF THE THREE-JET HEAVY QUARK PRODUCTION IN e^+e^- -ANNIHILATION: STATUS AND APPLICATIONS*

Mikhail Bilenky^{a†}, Germán Rodrigo^{b‡} and Arcadi Santamaria^c

^a Institute of Physics, AS CR, 18040 Prague and
Nuclear Physics Institute, AS CR, 25068 Řež(Prague), Czech Republic

^b INFN-Sezione di Firenze, Largo E. Fermi 2, 50125 Firenze, Italy

^c Departament de Física Teòrica, IFIC, CSIC-Universitat de València, 46100 Burjassot, València, Spain

Abstract

Next-to-leading order calculations for heavy quark three-jet production in e^+e^- annihilation are reviewed. Their applications for the measurement of the b-quark mass at LEP/SLC and for the test of flavour independence of the strong coupling constant are discussed.

*to be published in the Proceedings of the XXIX International Conference on High Energy Physics, Vancouver, B.C. Canada, July 23-29, 1998.

†On leave from JINR, 141980 Dubna, Russian Federation

‡On leave from Departament de Física Teòrica, IFIC, CSIC-Universitat de València, 46100 Burjassot, València, Spain

NLO CALCULATIONS OF THE THREE-JET HEAVY QUARK PRODUCTION IN e^+e^- -ANNIHILATION: STATUS AND APPLICATIONS

M. BILENKY

Institute of Physics, AS CR, 18040 Prague and Nuclear Physics Institute, AS CR, 25068 Řež(Prague), Czech Republic

G. RODRIGO

INFN-Sezione di Firenze, Largo E. Fermi 2, 50125 Firenze, Italy

A. SANTAMARIA

Departament de Física Teòrica, IFIC, CSIC-Universitat de València, 46100 Burjassot, València, Spain

Next-to-leading order calculations for heavy quark three-jet production in e^+e^- -annihilation are reviewed. Their applications for the measurement of the b-quark mass at LEP/SLC and for the test of flavour independence of the strong coupling constant are discussed.

1 Motivation

Effects of the bottom-quark mass, m_b , have been already noticed in the early tests¹ of the flavour independence of the strong coupling constant, α_s , in e^+e^- -annihilation at the Z^0 -peak. They became very significant in the final analysis, which included millions of hadronic Z^0 -decays^{2,3,4,5}. For example, if the b-quark mass is neglected, the ratio $\alpha_s^b/\alpha_s^{light}$, where α_s^b measured from hadronic events with b-quarks in the final state, and α_s^{light} from events with light quarks (uds), is shifted from one³ by 8%. Thus, high LEP/SLC precision requires an accurate account for the heavy quark mass^a in the theoretical predictions for the e^+e^- -annihilation into jets at the Z^0 -pole.

The quark mass effects in the Z^0 decays were discussed in the literature⁶. The leading order (LO) complete Monte-Carlo calculation for $e^+e^- \rightarrow 3jets, 4jets$ with massive quarks was first done in⁷. Later, motivated by the remarkable sensitivity of the three-jet observables to the value of the quark mass, the possibility of the determination of m_b at LEP, assuming universality of strong interactions, was considered^{8,9}. This question was analyzed in detail in⁹, where the necessity of the next-to-leading order (NLO) calculation for the measurements of the m_b was also emphasized.

The NLO calculations for the process $e^+e^- \rightarrow 3jets$, with complete effects of the quark mass, were performed independently by three groups^{10,11,12}. These predictions are in agreement with each other and were successfully used in the measurements of the b-quark mass far above threshold^{2,5} and in the precision tests of the universality

of the strong interactions^{2,3,4,5} at the Z^0 -pole^b.

In this talk we make a short review of next-to-leading order predictions for $e^+e^- \rightarrow 3jets$ including effects of the quark mass and its applications at the Z^0 -peak^c.

2 Why are the b-quark mass effects are significant in $Z^0 \rightarrow 3jets$?

It might seem surprising that at the Z^0 -pole, where the relevant scale is the Z^0 -boson mass, effects of the quark masses can not be neglected. Indeed, if one considers inclusive width of the decay $Z^0 \rightarrow \bar{b}b$, according to the Kinoshita-Lee-Nauenberg theorem there are no mass singularities, and the only way m_b enters calculations^d is in the ratio $\overline{m}_b^2(M_Z)/M_Z^2$. Therefore, quark mass effects in the best-measured observable for b-quarks are negligibly small $\sim 10^{-3}$.

But the situation is different in more exclusive processes. Let's consider the decay $Z^0 \rightarrow \bar{b}bg$, which contributes to the three-jet final state at the LO. This process has an infrared singularity in the limit when the energy of radiated gluon energy approaches zero. To make a physical prediction one has to introduce kinematical cuts. In the e^+e^- -annihilation this is usually done by applying one of the so-called jet clustering algorithms¹⁴. The phase-space for $Z^0 \rightarrow \bar{b}bg$ is split into two parts, two-jet and three-jet one, and this separation is defined by the jet-resolution parameter, y_c . Therefore, instead of two

^bDue to the large correlation between α_s and m_b , either m_b or α_s was treated as a free parameter. The value of another one was taken from other measurements.

^cWe would like to note that elements of these calculations can be also applied for the $e^+e^- \rightarrow \bar{t}t + \dots$.

^dTaking the \overline{MS} running quark mass one includes the principal part of the NLO QCD corrections to the total width^{13,9}.

^aIt is mainly related to the bottom-quark. Effects of the charm-quark mass are smaller, roughly by the factor m_c^2/m_b^2 .

scales in the inclusive process, M_Z and m_b , one has here in addition the new scale, $\sqrt{y_c}M_Z$. The jet-resolution parameter can be rather small, in the range $10^{-2} - 10^{-3}$ and effects of the quark mass appears as $m_b^2/(\sqrt{y_c}M_Z)^2$ and can reach several percents.

3 The three-jet observable

The convenient observable for studies of the mass effects in the three-jet final state is defined as follows

$$R_3^{bd} = \frac{\Gamma_{3j}^b(y_c)/\Gamma^b}{\Gamma_{3j}^d(y_c)/\Gamma^d} \quad (1)$$

$$= 1 + r_b \left(b_0(y_c, r_b) + \frac{\alpha_s}{\pi} b_1(y_c, r_b) \right) + \mathcal{O}(\alpha_s^2)$$

where Γ_{3j}^q and Γ^q are the three-jet and the total decay widths of the Z^0 -boson into a quark pair of flavour q , $r_b = m_b^2/M_Z^2$. Both the LO function, b_0 , and the NLO function, b_1 , depend on the jet-clustering algorithm. Note that although the leading r_b -dependence is factorized for convenience, the above expression is not an expansion in r_b .

This observable has both experimental and theoretical advantages. It is a relative quantity, therefore many experimental uncertainties due to the normalization drop out. In addition, in the ratios Γ_{3j}^q/Γ^q the bulk of electroweak corrections is cancelled. The double ratio (1) was measured by DELPHI² and used for the determination of the m_b . In practice one uses normalization with respect to all light flavours, uds . Such quantity then differs from R_3^{bd} , mainly due to the contribution of the triangle diagrams¹⁵. The difference is, however, very small numerically. Similar ratio normalized on $udsc$ was considered in¹¹.

Another observable is the differential two-jet rate, D_2 defined as

$$D_2^{bd} = \frac{[\Gamma_{2j}^b(y_c + \Delta y_c/2) - \Gamma_{2j}^b(y_c - \Delta y_c/2)]/\Gamma^b}{[\Gamma_{2j}^d(y_c + \Delta y_c/2) - \Gamma_{2j}^d(y_c - \Delta y_c/2)]/\Gamma^d} \quad (2)$$

with Δy_c taken to be sufficiently small. The two-jet width is obtained from the relation: $\Gamma_{2j}^q = \Gamma^q - \Gamma_{3j}^q - \Gamma_{4j}^q$, where Γ_{4j}^q is the four-jet width.

Different event shapes observables were considered^{12,11,3} in the literature as well.

4 The leading order calculation

The LO contribution to the decay $Z^0 \rightarrow 3jets$ is given by the process $Z^0 \rightarrow b\bar{b}g$. At the LO we can not specify what value of m_b should be taken in the calculations: all definitions of the quark mass are equivalent (the difference is due to the higher orders in α_s). One

can use^e, for example, the pole mass $M_b \approx 4.6GeV$ or the \overline{MS} -running mass $\overline{m}_b(\mu)$ at any scale relevant to the problem, $m_b \leq \mu \leq M_Z$, with $\overline{m}_b(m_b) \approx 4.13GeV$ and $\overline{m}_b(M_Z) \approx 2.83GeV$.

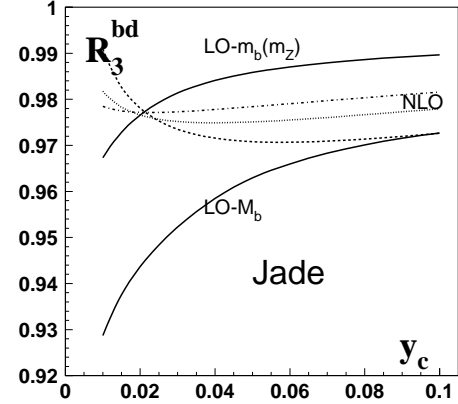


Figure 1: The ratio R_3^{bd} (Jade) as a function of y_c .

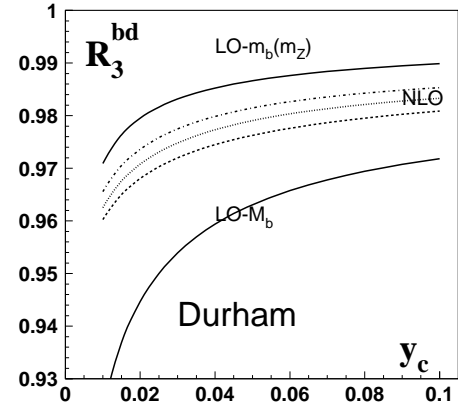


Figure 2: The ratio R_3^{bd} (Durham) as a function of y_c .

The results for the ratio R_3^{bd} , Eq.(1), for Jade¹⁷ and Durham¹⁸ schemes are presented by solid curves in the Figs.1,2. The upper curve corresponds to $m_b = 2.83GeV$, the lower one to $m_b = 4.6GeV$. The difference between the two curves gives the size of the uncertainty of the LO prediction. To improve the situation the NLO calculation is necessary.

It is worth mentioning that the residual mass dependence in the function $b_0(y_c, r_b)$ is small in the region $0.005 < y_c < 0.1$, especially for the Durham scheme. The simple interpolation: $b_0 = b_0^{(0)} + b_0^{(1)} \ln y_c + b_0^{(2)} \ln^2 y_c$ can be used in practice^{9,19}.

^eThe values of the b-quark masses are taken from the recent sum rules and lattice QCD analyses¹⁶ of the Υ and B mesons spectra.

5 The next-to-leading order corrections

At the NLO there are two different contributions. One comes from one-loop corrections to the three-parton decay, $Z^0 \rightarrow b\bar{b}g$. Another one comes from tree-level four-parton decays $Z^0 \rightarrow b\bar{b}gg$ and $Z^0 \rightarrow b\bar{b}q\bar{q}$, $q = u, d, s, c, b$ integrated over the three-jet region of the four-parton phase-space. The main difficulty of the NLO calculation is the presence of ultraviolet (UV) and infrared (IR) divergences at the intermediate stages. The UV divergences in the one-loop part are removed by renormalization of the QCD parameters. The IR singularities in the virtual part are due to massless gluons in the loops. In the four-parton process they appear when one of the gluons is soft or two gluons are collinear. The sum of the virtual and tree-level contributions is, however, IR finite. In addition, the finite quark mass makes the NLO calculation technically much more involved, comparing to the massless one, known since many years^{20,21}.

The one-loop part is calculated analytically and dimensional regularization is used to regularize both UV and IR divergences. The IR singularities appear as simple and double poles in ϵ , $D = 4 - 2\epsilon$, where D is space-time dimension. The singular part is proportional to the tree-level transition probability and it is cancelled by the IR-singular part of the four-parton contribution.

There are several methods of analytical cancelation of IR singularities. In^{10,11} the so-called slicing method²² was used. In this case the analytical integration over a thin slice at the border of phase-space is performed in D -dimensions. The integration over the rest of the phase-space, defined by a particular jet-algorithm, is done numerically in $D = 4$. In the third NLO calculation¹², a different approach, the so-called subtraction method (see e.g.^{20,23}) was used.

We would like to stress that the structure of the NLO result for the $Z^0 \rightarrow 3\text{jets}$ in the massive case is completely different from the massless one^{20,21}. In the massive case the collinear divergences associated with the gluon radiation from the quarks, are softened into $\ln r_b$ and only collinear divergences due to gluon-gluon splitting remain. Therefore, the test performed in¹⁰ by recovering the massless limit from the result with finite mass, is a rather non-trivial one.

In contrast to the LO function, b_0 , the NLO function b_1 has a significant residual mass dependence^{10,19} and the phenomenological interpolation, e.g. for Durham scheme, can be chosen as follows

$$b_1 = b_1^{(0)} + b_1^{(1)} \ln y_c + b_1^{(2)} \ln r_b . \quad (3)$$

The approximation Eq.(3) works well in the region $0.01 \leq y_c \leq 0.1$ and extra powers of $\ln r_b$ and/or mixed terms $\ln r_b \ln y_c$ do not improve its quality.

In the NLO calculations one can, and have to, specify the quark mass definition. It turned out that technically it is simpler to use a mixed renormalization scheme with on-shell definition for the quark mass and \overline{MS} definition for the strong coupling. In this case observables are originally expressed in terms of the pole mass. This definition of the quark mass can be perfectly used in perturbation theory. However, in contrast to the pole mass in QED, the quark pole mass is not a physical parameter. The non-perturbative corrections to the quark self-energy bring an unavoidable ambiguity of order $\approx 300\text{MeV}$ (hadron size) to the physical position of the pole of the quark propagator²⁴. Above the quark production threshold, it is natural to use the running mass definition (we use \overline{MS}). The advantage of this definition is that $\overline{m}_b(\mu)$ can be used for any scale, $\mu \gg m_b$. The pole, M_b , and the running masses of the quark are perturbatively related

$$M_b = \overline{m}_b(\mu) \left[1 + \frac{\alpha_s}{\pi} \left(\frac{4}{3} - \ln \frac{m_b^2}{\mu^2} \right) \right] . \quad (4)$$

Although this relation is known to higher orders in α_s , we use its one-loop version to pass from the pole mass to the running one, which is consistent with NLO calculations.

Substituting Eq.(4) into Eq.(1) we have

$$R_3^{bd}(y_c, \overline{m}_b(\mu), \mu) = 1 + \overline{r}_b(\mu) \left[b_0 + \frac{\alpha_s(\mu)}{\pi} \left(\overline{b}_1 - 2b_0 \ln \frac{M_Z^2}{\mu^2} \right) \right] \quad (5)$$

with $\overline{b}_1 = b_1 + b_0(8/3 - 2 \ln r_b)$ and $\overline{r}_b = \overline{m}_b^2/M_Z^2$.

To relate quark masses at different scales, we use the one-loop renormalization group equation, e.g. $\overline{m}_b(\mu) = \overline{m}_b(M_Z) \left[\frac{\alpha_s(\mu)}{\alpha_s(M_Z)} \right]^{\frac{2\gamma_0}{\beta_0}}$, where $\gamma_0 = 2$ and $\beta_0 = 11 - \frac{2}{3}n_f$ with $n_f = 5$.

6 Numerical results and discussion.

In Figs.1,2 we show NLO results, obtained by using Eq.(5) parameterized in terms of $\overline{m}_b(M_Z) = 2.83\text{GeV}$ for different values of the renormalization scale $\mu = 10\text{GeV}$ - dashed line, $\mu = 30\text{GeV}$ - dotted line and $\mu = M_Z$ - dashed-dotted line. As expected, the NLO curve for large scale is closer to LO curve for $\overline{m}_b(M_Z)$, while NLO result for smaller scale is closer to the LO one for M_b . Like in the massless case¹⁴, the NLO corrections for the Jade scheme are larger than in the Durham and depend significantly on y_c for small values, $y_c < 0.025$.

The μ -dependence is a reflection of the fixed order perturbative calculation and the size of the variation of the observable is usually used to estimate higher order corrections. The study of the μ -dependence for the Durham scheme is presented in Fig.3. The R_3^{bd} is shown as a function of scale μ for the fixed value of $y_c = 0.02$.

The lower, solid curve is obtained by using Eq.(1), i.e. parameterized in terms of the pole quark mass. In this case the scale dependence is due to the renormalized coupling constant, α_s . Other curves show μ -dependence when R_3^{bd} is parameterized in terms of the running mass, $\overline{m}_b(M_Z)$, Eq.(5), with different definitions of the quark mass used in the logarithms: M_b , $\overline{m}_b(M_Z)$, $\overline{m}_b(\mu)$.

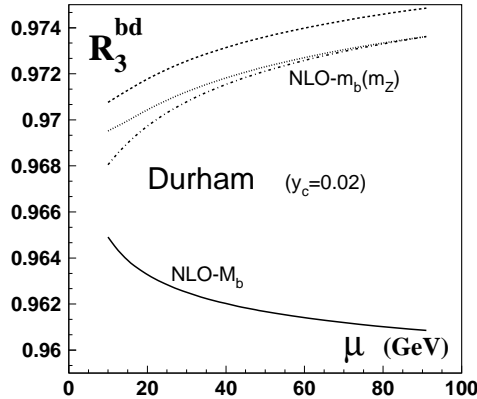


Figure 3: The ratio R_3^{bd} (Durham) as a function of μ .

The conservative estimate^f of the theoretical error for the R_3^{bd} is to take the whole spread given by the curves in Fig.3. The uncertainty in R_3^{bd} induces an error in $\overline{m}_b(M_Z)$: $\Delta R_3^{bd} = 0.004 \rightarrow \Delta m_b \simeq 0.23 \text{ GeV}$, which is, however, below current experimental errors, dominated by fragmentation.

In the Figs.4,5 we show results for the fixed value of scale, $\mu = M_Z$, for the Cambridge algorithm²⁵, a recently proposed modification of the Durham scheme.

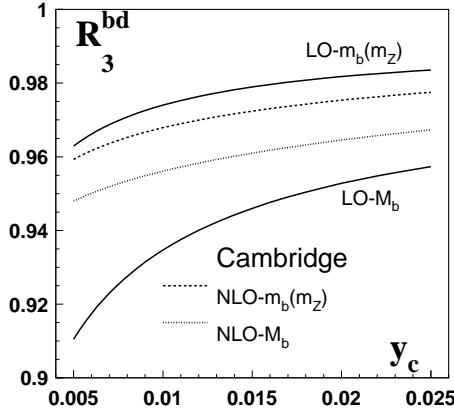


Figure 4: The ratio R_3^{bd} (Cambridge) as a function of y_c .

It is remarkable that in this scheme and for two observables, R_3^{bd} and two-jet differential ratio, D_2 (see Eq.(2)), the LO result for the running mass, $\overline{m}_b(M_Z)$ is very close to the NLO one. In a sense, it is similar to

^fThe Jade scheme gives significantly larger error, see Fig.1.

the total width: the main radiative corrections are taken into account by the running of the QCD parameters to the M_Z -scale. Note also that for small, but still reasonable value of $y_c \approx 0.01$, the mass effects in D_2 are as large as 10% (although one has to remember that this is a differential rate and statistical errors are larger here too).

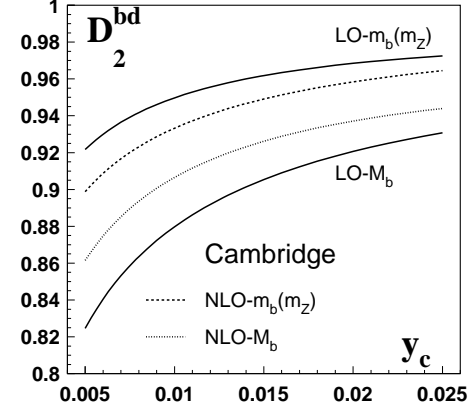


Figure 5: The ratio D_2^{bd} (Cambridge) as a function of y_c .

The scale dependence for the Cambridge scheme is shown in Fig.6 for fixed $y_c = 0.01$. The result is also quite remarkable. The ratio expressed in terms of running mass is very stable with respect to scale variation. This behavior in the Cambridge scheme is rather promising with respect to improvements of the DELPHI result² for $\overline{m}_b(M_Z)$. We refer to²⁶ for detailed discussion of the NLO predictions in this new scheme and to²⁷ for the first analysis of the LEP data applying the Cambridge algorithm.

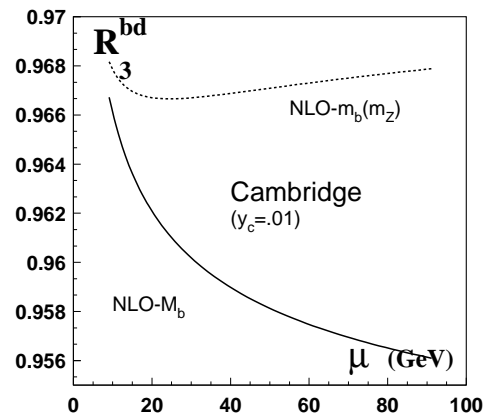


Figure 6: The ratio R_3^{bd} (Cambridge) as a function of μ .

7 Conclusions

Three-jets observables at the Z^0 -peak (jet rates, differential jet-rates, event-shape observables etc.) have sig-

nificant mass effects ranging up to the 10% depending on the observable, jet algorithm and the value of the jet resolution parameter. This requires accurate theoretical input, including mass effects, for tests of the flavour independence of the strong interactions and measurements of the bottom-quark mass.

In the last years an important progress was done in the description of the decay Z^0 into three-jet with massive quarks. The next-to-leading calculations have been done by three groups and have been successfully used in the analysis of the LEP and SLC data. The NLO corrections are in the range of 1 – 3% and are within the experimental reach. Further studies of different observables and different jet-algorithms are oriented on the reduction of the theoretical uncertainty. One good candidate might be the Cambridge jet-algorithm, where the NLO corrections are particularly small and where the predictions in terms of the running mass, $m_b(M_Z)$ are particularly stable with respect to the variation of the renormalization scale.

Acknowledgments

We are very pleased to thank S. Cabrera, J. Fuster and S. Martí for an enjoyable collaboration.

References

1. L3 Coll., B. Adeva, et al., *Phys. Lett. B* **263**, 551 (1991); DELPHI Coll., P. Abreu, et al., *Phys. Lett. B* **307**, 221 (1993); OPAL Coll., R. Akers, et al., *Z. Phys. C* **65**, 31 (1995); ALEPH Coll., D. Buskulic et al., *Phys. Lett. B* **355**, 381 (1995); SLD Coll., K. Abe et al., *Phys. Rev. D* **53**, 2271 (1996).
2. DELPHI Coll., P. Abreu, et al., *Phys. Lett. B* **418**(1998)430; J. Fuster, S. Cabrera and S. Martí, *Nucl. Phys. Proc. Suppl.* **54A**(1997)39.
3. OPAL Coll., see D. Chrisman in *QCD98*, ed. S. Narison *Nucl. Phys. Proc. Suppl.*, to appear.
4. SLD Coll., K. Abe et al., hep-exp/9805023.
5. P.N. Burrows, review of DELPHI, OPAL and SLD results, these Proceedings.
6. For review see: L.J. Reinders, H. Rubinstein and S. Yazaki, *Phys. Rep.* **127** (1985) 1; J.H. Kühn and P.M. Zerwas, *Phys. Rep.* **167** (1988) 321
7. A. Ballestrero, E. Maina, S. Moretti, *Nucl. Phys. B* **415**, 265 (1994) and *Phys. Lett. B* **294**, 425 (1992).
8. J. Fuster, private communications
9. M. Bilenky, G. Rodrigo, and A. Santamaria, *Nucl. Phys. B* **439**(1995)505.
10. G. Rodrigo, A. Santamaria and M. Bilenky, *Phys. Rev. Lett.* **79**(1997)193, hep-ph /9703360 and hep-ph/9802359; G. Rodrigo, hep-ph/9703359 and *Nucl. Phys. Proc. Suppl.* **54A**(1997)60;
11. W. Bernreuther, A. Brandenburg and P. Uwer, *Phys. Rev. Lett.* **79** (1997) 189; A. Brandenburg and P. Uwer, *Nucl. Phys. B* **515** (1998) 279.
12. P. Nason and C. Oleari, *Phys. Lett. B* **407** (1997) 57 and *Nucl.Phys.* **B521**(1998)237; C. Oleari, hep-ph/9802431.
13. A. Djouadi, J. H. Kühn and P. M. Zerwas, *Z. Phys. C* **46**(1990)411; K. G. Chetyrkin and J. H. Kühn, *Phys. Lett. B* **248**(1990)359.
14. For review see: S. Bethke et al., *Nucl. Phys. B* **370**, 310 (1992); S. Moretti, L. Lonnblad and T. Sjöstrand, hep-ph/9804296.
15. K. Hagiwara, T. Kuruma and Y. Yamada, *Nucl. Phys. B* **358**, 80 (1991).
16. For recent low energy determinations of b-quark mass see e.g.: M. Jamin and A. Pich in *QCD98*, ed. S. Narison *Nucl. Phys. Proc. Suppl.*, to appear and *Nucl. Phys. B* **507** (1997) 334; V. Giménez, G. Martinelli and C.T. Sachrajda, *Phys. Lett. B* **393**(1997)124;
17. JADE Coll., W. Bartel et al., *Z. Phys. C* **33**, 421 (1981).
18. S. Catani et al., *Phys. Lett. B* **269**, 432 (1991).
19. M. Bilenky, G. Rodrigo and A. Santamaria, in *QCD98*, ed. S. Narison *Nucl. Phys. Proc. Suppl.*, to appear.
20. R.K. Ellis, D.A. Ross and A.E. Terrano, *Nucl.Phys. B* **178**(1981)421;
21. J.A.M. Vermaasen, K.J.F. Gaemers and S.J. Oldham, *Nucl. Phys. B* **187**(1981)301; K. Fabricius et al., *Z. Phys. C* **11**(1981)315
22. F. Gutbrod, G. Kramer and G. Schierholz, *Z.Phys.C* **21** (1984) 235. H. Baer, J. Ohnemus, and J. F. Owens, *Phys.Rev.D* **40** (1989) 2844; F. Aversa et al., *Phys.Rev.Lett.* **65** (1990) 401; W. T. Giele and E. W. N. Glover, *Phys.Rev.D* **46** (1992) 1980; W. T. Giele, E. W. N. Glover and D. A. Kosower, *Nucl.Phys.B* **403** (1993) 633;
23. Z. Kunszt and P. Nason, in *Z Physics at LEP 1*, ed. G. Altarelli, R. Kleiss and C. Verzegnassi, CERN 89-08, 1989.
24. I.I. Bigi et al., *Phys. Rev. D* **50**, 2234 (1994); M. Beneke and V.M. Braun, *Nucl. Phys. B* **426**, 301 (1994).
25. Y.L. Dokshitser et al., *JHEP* **08** (1997) 1.
26. G. Rodrigo, A. Santamaria and M. Bilenky, hep-ph/9807489.
27. DELPHI Coll., J. Fuster, S. Cabrera and S. Martí, contributing paper #152 to the ICHEP98 Conf.